SATURATION DISTRIBUTIONS IN HEAVY OIL RESERVOIRS

by

Joshua Todd Staten

A thesis submitted to the faculty of
The University of Utah
in partial fulfillment of the requirements for the degree of

Master of Science

Department of Chemical Engineering

The University of Utah

December 2016

The University of Utah Graduate School

STATEMENT OF THESIS APPROVAL

The thesis of **Joshua Todd Staten**

has been approved by the following supervisory committee members:

Milind Deo	, Chair	**10/27/2016** Date Approved
Jules J. Magda	, Member	**10/27/2016** Date Approved
Richard Roehner	, Member	**10/27/2016** Date Approved

and by **Milind Deo** , Chair of

the Department of **Chemical Engineering**

and by David B. Kieda, Dean of The Graduate School.

ABSTRACT

Models that describe conventional reservoirs can be used to explore the possibility of heavier-than-water oil. Steam-assisted gravity drainage (SAGD) is a common process in reservoirs with extra heavy oils (oil sands). In some cases, oil that is heavier than water is present in these reservoirs. The segregation of oil and water may cause issues for recovery. It is important to understand the initial saturation distribution of oil and water for proper design of injection. It was found through simulation that the heavy oil would pool towards the bottom of a heavy oil reservoir with water remaining on top of the oil. With capillary pressure, the heavy oil and water will form a transition zone. The extent of the transition zone is dependent on the density gradient of the oil, the density difference between the oil and water, and the slope of the capillary pressure saturation profile. This finding influences the positioning of production piping in steam-assisted gravity drainage (SAGD) as well as possible geological pooling areas for recovery. The possibility of a water zone between oil zones increases the risk of missing oil in the reservoir when drilling or perforating.

TABLE OF CONTENTS

LIST OF FIGURES

Figures

ACKNOWLEDGEMENTS

With gratitude for all of the assistance, I give thanks to my advisor, Milind Deo, my committee, J. Magda and Rich Roehner, and ConocoPhillips for technical and logistical aid. I give thanks to my family and friends for helping me keep completion in the forethoughts of my mind.

CHAPTER 1

INTRODUCTION

Transportable energy drives economy, industry, and technology (Hondroyiannis, Lolos, and Papapetrou 2002). Oil and natural gas are major energy sources that influence an overall energy portfolio (*Annual Energy Review 2011*, 2012). Economics and environmental impact are two standards against which each energy source is measured (National Renewable Energy Laboratories 2015). There is public demand for cheaper and more environmentally friendly energy, but the two standards are often in opposition (Tidball, Bluestein, Rodriguez, and Knoke 2010). Technology acts as a mediator between cost and environmental impact; in other words, better technology can lower the cost of energy and lessen the environmental impact. Heavy oil and bituminous oil in most cases are less favorable economically and environmentally in comparison to conventional light sweet crude, but the diminishing conventional crude oil supply, advances in technology, and higher oil prices have spurred development of heavier and more bituminous resources. New energy sources are needed to fill a void that is being left by diminishing conventional sources, but the new sources must meet economic and environmental standards.

An example of how economical and to a lesser extent environmental

demands have been met through technology is the shale oil boom, which is producing sweet light crude in quantities that have exceeded most expectations (US Energy Information Agency 2013). The development of shale oil has drastically overshadowed the heavy oil development in Canada and California, but thermally assisted enhanced oil recovery is still a major source of oil.

As oil production transitions from conventional resources to unconventional resources, technological improvements are needed for better recovery factors. Unconventional sources will become the new convention if technology creates equally favorable economics as present conventional resources. Research and technology work together to gain insight into the physical phenomena that control the ability to produce the oil. The end goal of the research and technology in heavy oil systems is to create a low-priced, sustainable, and transportable energy that can be sold for profit with little impact on the environment. Thus far, the research is not there. One issue that remains clouded by the complexities of heavy oil systems is how saturation varies with depth.

The energy that is harvested in oil and gas systems is ultimately from solar energy that was captured and consumed by organisms that lived millions of years ago. Those organisms died and sank to the depths of a marine environment. Before the proteins and carbohydrates decomposed, they were buried in an anoxic environment with detritus from millions of years of erosion. As burial depth increased, temperature and pressure increased. The chemicals polymerized, forming kerogen. Sediments continued to bury the kerogen. The

kerogen reached a temperature at which it was no longer stable and began to break down (catagenesis), forming bitumen and lighter oleic compounds. Further temperature maturation of bitumen yields oil and gas on a continuum; in other words, bitumen is the least thermally mature and gas is the most thermally mature. The bitumen and other oleic compounds still contain much of the energy that was originally captured by organisms. Some of the oleic compounds move from the maturing kerogen-rich shales into a reservoir. Charging the reservoir with oil and gas requires enough force in the oleic phases to drain the water from the reservoir and replace it. The amount of water left in the reservoir is dependent on the oleic, aqueous, and rock force balance. Buoyancy, capillarity, pressure, and chemical potential contribute to the movement of oleic compounds from organic-rich shale to a reservoir. At one time, bituminous reservoirs generally had their light ends, but had them removed by biodegradation, water washing, or multiple charging (Head, Gray, and Larter 2014; Hein, Leckie, Larter, et al. 2013).

For bituminous reservoirs, energy must be added (enhanced oil recovery) to the bitumen to increase its temperature thereby reducing its viscosity for extraction. Additional capital and operating expenses make bituminous reservoirs riskier as an investment, but also create more potential for gains from optimization and technological advances. Research is conducted in many areas that may lead to improvement in economic recovery. One area of research that may lead to a more favorable economic recovery is saturation variation with depth due to capillary pressures.

Water saturation, grain size, and grain type are interconnected factors that contribute to the mobility/recovery of the oil. Other factors of mobility are dependent on oil characteristics, such as viscosity. The water-oil-rock relationship is essential in determining whether the reservoir will be economical to produce. Modeling these factors is a less risky method of determining economic benefit than developing a source without modeling.

Saturation variation with depth is overlooked in conventional reservoirs because the heterogeneity, in such reservoirs, blurs the full impact of the capillary pressure effects on saturation. As models are developed to describe the heterogeneity factors in reservoirs, the saturation variation will become more powerful in describing the reservoir.

Oil saturation and water saturation are average volumetric fractions of oil and water in the pores of the reservoir rock. Water occupies a volume of pore space and oil resides in the balance. If there is free gas present, then the gas volume is also taken into consideration when calculating the saturations. Oil saturation varies with depth in the reservoir. Conventional reservoirs, oil reservoirs with oil lighter than water and good oil mobility without stimulation, have a transition zone where oil saturation decreases as depth increase. Research into whether heavy oil transition zones are similar to conventional sources is lacking.

1.1 Purpose

The purpose of this paper is to describe a developed model that predicts how petroleum saturation varies with reservoir depth in heavy oil reservoirs. Understanding the variation with depth will enable service and energy companies to create better plans for drilling and producing their reservoirs (i.e., planning to perforate at a depth in which the petroleum properties are most ideal for flow or ultimate recovery). The model will also provide service and energy companies with a more accurate estimated ultimate recovery (EUR) for their modeled reservoirs. With better estimates of ultimate recovery and more optimized drilling and producing techniques, more money will be made per well and fewer resources will be wasted.

The developed model is applicable to most heavy oil reservoirs. The model gives a rough estimate of the saturations at different depths within the reservoir. However, the model is highly dependent on the information gathered on the reservoir in question. If maximum accuracy is needed, then the reservoir rock and fluid characteristics must be well defined. The model was developed to give a general estimate of saturations in the transition zones of heavy oil reservoirs.

1.2 Vertical Equilibrium

Research in oil recovery from tar sands, shale oil/gas, oil shale, and other unconventional oil sources is cyclical. The cycles of research follow the crude oil prices; when crude oil prices are high, theoretical research is funded with fervor.

When crude oil prices are low, applied research is meagerly funded and little to no funding is granted for theoretical research in unconventional sources.

Initial research on vertical equilibrium in oil reservoirs was performed by Muskat (1930), who incorrectly reasoned that effects of gravity would be minimal for practical heights above the gas-oil contact (GOC) (Muskat 1930). Sage and Lacey (1938) faulted Muskat's assumption that temperature, pressure, and composition were not coupled and then showed that gravity has significant effects on composition (Sage and Lacey 1939). Leverett (1940) introduced the idea that capillarity affects the static and dynamic balance of fluid densities in porous media (Leverett 1940).

Research on vertical equilibrium was sparse for many years, then Coats, Dempsey, and Henderson (1971) reopened the discussion with a seminal paper on modeling and simulating heterogeneous reservoir behavior. They concluded that new computing power made heterogeneous treatment of reservoirs viable. They also provided a quick check method for an a priori appraisal for vertical equilibrium. With production in the Brent field of the North Sea, the effort to describe vertically dependent compositions that had been on hiatus for many years was redoubled. The Brent field is unique because it has large transition zones. Schulte (1980) solved for compositional gradients, such as gradients of the Brent field, by using the Peng-Robinson equation of state and classic thermodynamic theory (Schulte 1980). Schulte was one of the first to use a cubic equation of state to solve for reservoir compositional gradients. Wheaton (1988) presented a thermodynamic theory and formula including capillary pressures to

calculate compositions at different depths (Wheaton 1991). Lee (1989) took Wheaton's work one step further by adding interfacial curvature effects to the thermodynamic calculations, thereby allowing the theory to model two phases within the reservoir (Lee 1989). Whitson and Belery (1994) compiled many previous works and introduced an algorithm that can be used to step vertically through a reservoir solving, by using fugacity as an intermediate factor, for pressure and composition at each height (Whitson and Belery 1994). Høier, Whitson, and Pera (2001) reviewed all current practices for modeling compositional grading of reservoirs (Høier, Whitson, and Pera 2001). Sedaghat, Daliri, and Mohammadi took Whitson and Belery's work from 1994 and improved the algorithm making the convergence faster and less computationally intensive (Sedaghat, Daliri, and Mohammadi 2013).

1.3 Saturation Functions

Saturation functions are needed for modeling and understanding fluid behavior in reservoirs. Leverett correlated many reservoirs' capillary pressure data by nondimensionalizing factors (as seen in Eq. 9). His nondimensional *J*-function is used mainly to scale capillary pressure functions from one set of porosity and permeability to another (Leverett 1940). Gerhard and Keuper studied capillary characteristics of saturated porous media using constitutive relationships for drainage from Brooks and Corey (Brooks and Corey 1964) and van Genuchten (van Genuchten 1980; Gerhard and Kueper 2003). Critics have argued that more factors are needed to accurately scale capillary pressure

functions in reservoirs (El-Khatib 1995; Phelps 1993). Sarwaruddin, Skauge, and Torsaeter took the Leverett *J*-Function and modified it to incorporate pore size distribution, irreducible liquid saturation, and tortuosity to provide a more general capillary pressure equation (Sarwaruddin, Skauge, and Torsaeter 2001).

1.4 Summary

The previous modeling work has progressed over the years getting more precise, but more complicated. Vertical equilibrium models describe the reservoir system, but the details can become more complicated than needed. Equations of state for liquids become less accurate the more complex the components in the system. Capillary pressure functions are difficult to transfer from one reservoir to another. There is a need for better understanding of the primary factors, such as capillary pressure, in reservoirs before the small changes in accuracy seen in the introduction of other factors can be a benefit. The progression in modeling conventional reservoirs hasn't been fully transferred into unconventional resources. Effects of capillary pressure in heavy oil resources have the potential to explain the compositional gradients in heavy oil reservoirs. This thesis furthers the understanding of capillary pressure functions on the saturation profile of heavy oil reservoirs and can be used in the application of oil recovery.

CHAPTER 2

MODELING AND ASSUMPTIONS

The model describes capillary pressure and water saturation during an initialization step in a reservoir simulator. In constructing the model, three factors were explored to ensure precision and accuracy: capillarity, saturation, and pressure. A flowchart shown in Figure 1 describes the algorithm used in the model. The inputs for densities of water, oil, and gas can be specific values or equations that describe the density variation with depth and pressure. Once the capillary pressures are calculated at each depth, a relationship of capillary pressure and saturation is used to calculate the saturations at each depth.

The change in free energy of a finite volume of water is zero when the fluids have reached capillary-gravity equilibrium. The two forces on a fluid if that fluid is moved within the vertical column are represented by the Eqs. 1–4.

$$dE_f = \frac{\partial E_f}{\partial h} dh + \frac{\partial E_f}{\partial P_w} dP_w \quad \text{.....(1)}$$

$$\frac{\partial E_f}{\partial h} = \rho_w g \Delta V \quad \text{.....(2)}$$

$$\frac{\partial E_f}{\partial P_w} = \Delta V \quad \text{.....(3)}$$

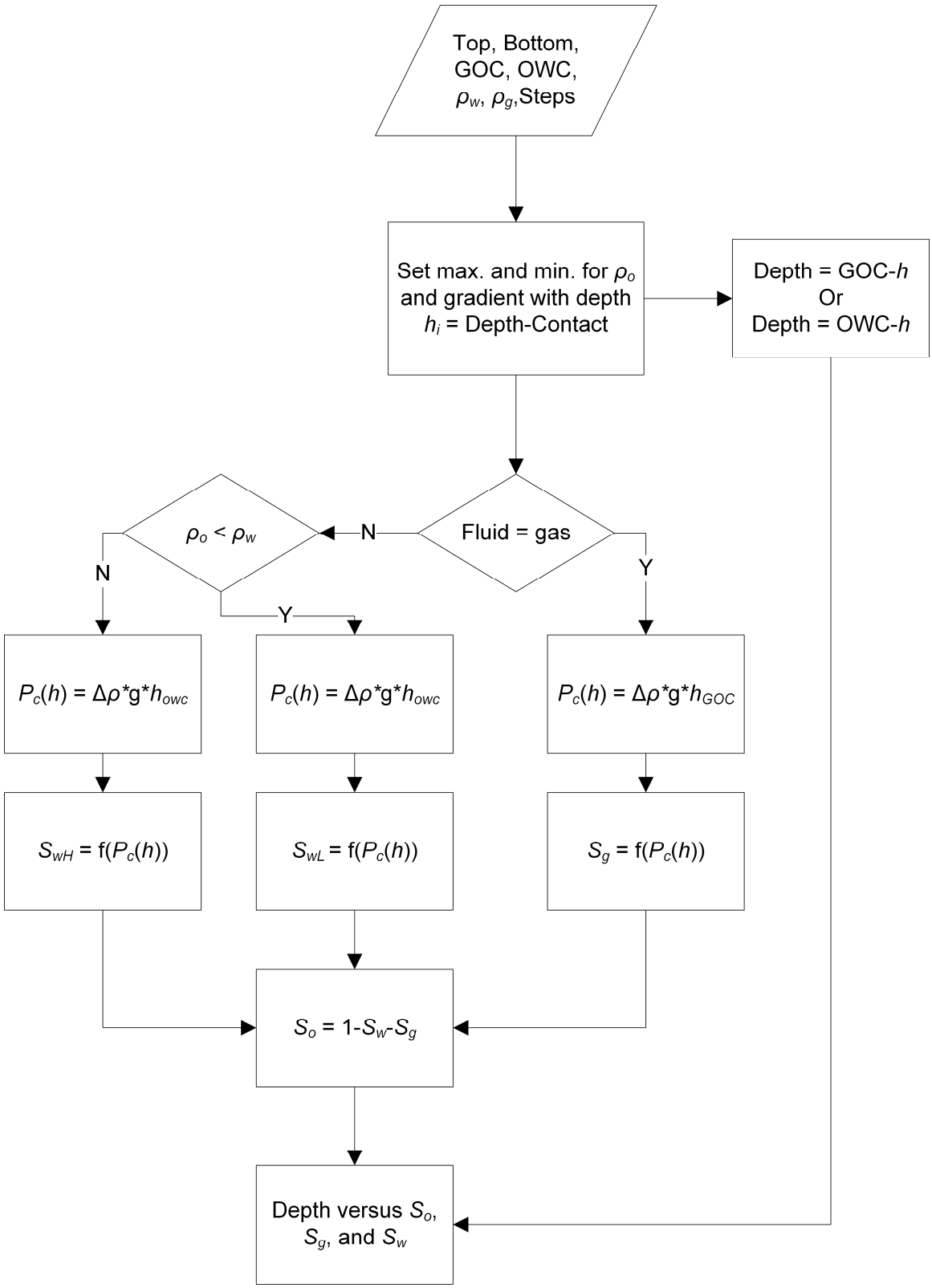

Figure 1: Oil Saturation Algorithm Flowchart. The user enters the depth of the gas-oil contact (GOC), the oil-water contact (OWC), and the densities (ρ_i). Equations are described in the Theory/Calculations section.

$$dE_f = \rho_w g \Delta V dh + \Delta V dP_w = 0 \quad (4)$$

where E_f is the fluid's free energy and h is the height of the fluid above the level, g is gravity, ρ is the density of water, V is the volume, and P_w is the phase pressure of water.

Phase pressures in a reservoir are dependent on the hydrostatic and capillary pressures. Eq. 5 and Eq. 6 are the phase pressure equations for water and oil, respectively. Capillary pressure can be calculated from phase pressures (Eq. 7).

$$-dP_w = \rho_w g dh \quad (5)$$

$$-dP_o = \rho_o g dh \quad (6)$$

$$P_c = P_o - P_w \quad (7)$$

where ρ_w is the density of water, ρ_o is the density of oil, g is gravity, d is the depth of continuous vertical column at which the phase pressure is being calculated, and P_c is the capillary pressure at the same depth. These equations assume a continuous water column. Depending on the information that is available on the reservoir, another method may be used to calculate P_c, as seen in Eq. 8.

Figure 2 shows the application of Eqs. 5, 6, and 7 in a reservoir with an oil density gradient. Phase pressure increases continuously with depth but capillary pressure is dependent on the height above or below the oil-water contact.

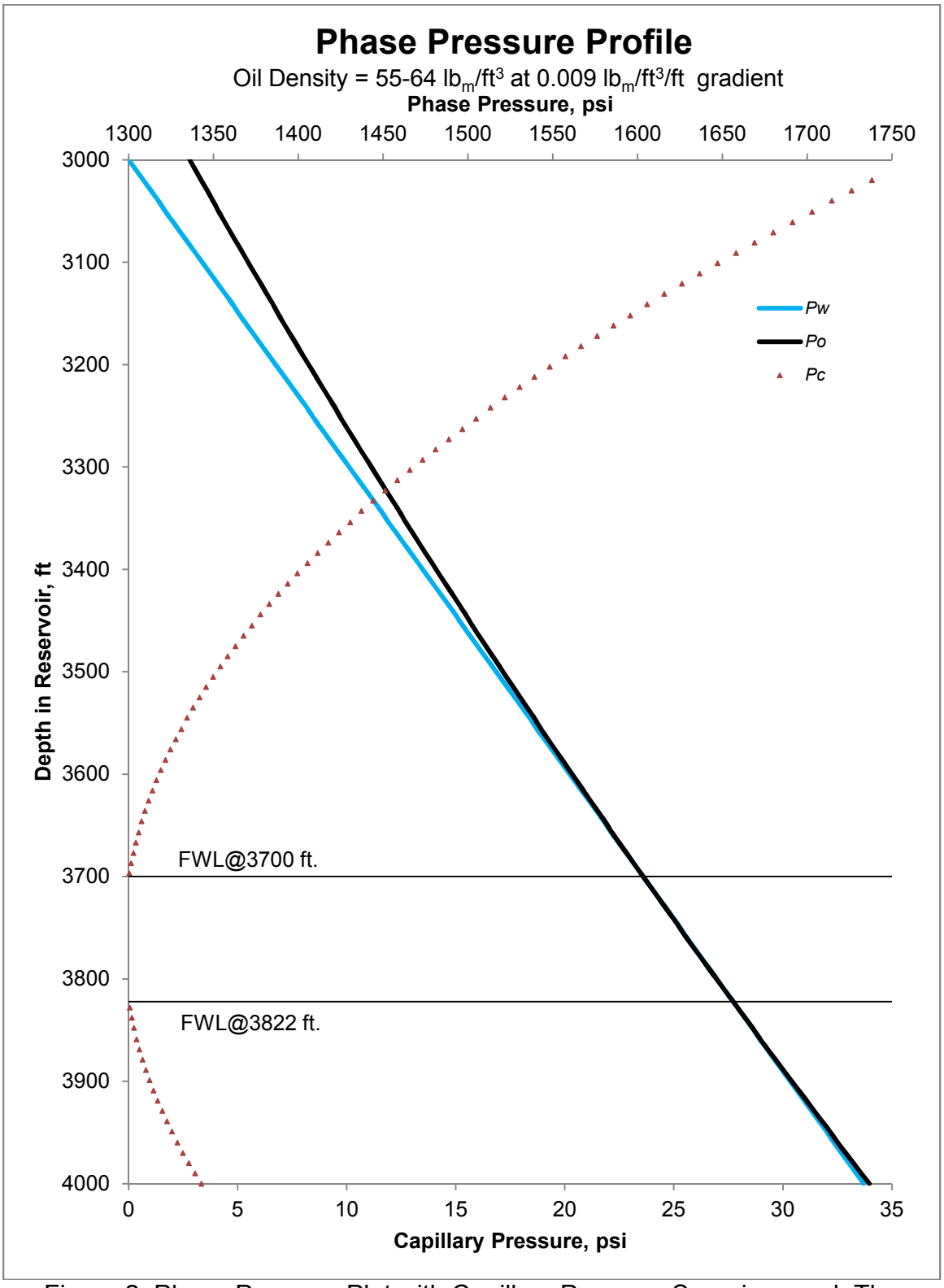

Figure 2: Phase Pressure Plot with Capillary Pressure Superimposed. The depths where the capillary pressure is zero are the free water levels (FWL) for lighter-than-water oil (3700 ft) and heavier-than-water oil (3822 ft) as the oil density changes linearly with depth.

The phase pressure profiles that are seen in Figure 2 have points where the two curves intersect in the phase pressure plot that indicates an oil-water contact. These points are reflected in the capillary pressure curve where the capillary pressure is zero. Zero capillary pressure points are important because they signify that there is a break of continuity in one of the phases. A negative capillary pressure zone is observed when the oil phase pressure is less than the water phase pressure. The negative capillary pressure indicates that the oil is being repelled from the zone due to the thermodynamic relationship between oil and water and therefore the oil saturation in this zone is suppressed to the residual oil saturation that was accumulated during migration and charging of the reservoir.

Using Eq. 7, Eq. 8 can be derived. The capillary pressure can be found empirically, but it is dependent on the saturation of the water. Eq. 8 takes the empirical and combines it with the theoretical for a semi-empirical model. Eq. 9 uses Eq. 8 and other characteristics between the rock and water for a nondimensional model that can be applied to relate reservoirs of similar rock type.

$$P_c(S_w) = (\rho_w - \rho_o) g h_{owc} \quad \text{.....(8)}$$

$$J = \frac{P_c(S_w)}{\sigma \cos\theta} \sqrt{k/\phi} \quad \text{.....(9)}$$

where S_w is the water saturation, ρ_w and ρ_o are water and oil densities, respectively, and h_{owc} is the distance from the oil-water contact.

The third and final method discussed herein is the Leverett *J*-function, as seen in Eq. 9. Where J is an empirical correlation function of saturation and capillary pressure determined from laboratory tests, σ is the interfacial tension between oil and water, θ is the contact angle between the water and the rock, k is the absolute permeability of the rock, and ϕ is the porosity of the rock. The empirical correlation function varies for each reservoir because it is dependent on rock and fluid properties (e.g., it is different for a limestone reservoir when compared to a sandstone reservoir).

Fluid saturations in the pore space range from 0 to 1 for each of the components. The saturations are coupled in that the sum of the saturations must be 1 and that each saturation must be between 0 and 1. Phase pressure in the pore is a determining factor for phase saturation. Equations for the calculation of the phase pressure can be seen in Eqs. 5 and 6. The major difference between the two equations is the capillary pressure. Determining capillary pressure is done through experiment. A saturation-capillary pressure profile is found through core experiments and then modeled to predict the reservoir saturation. Most reservoirs have their own empirical models and correlations, but some common fitting equations have been researched through the years (Gerhard and Kueper 2003).

This paper uses some simple saturation-capillary pressure models that demonstrate some core intuition about how the saturation-capillary pressure profile affects the saturation-depth profile.

S_w, S_{wirr}, p_d, λ, m_d, n_d, and α_d are water saturation, irreducible water

saturation, displacement pressure, and other fitting parameters, respectively.

$$P_c1(S_w) = -2 * S_w + 2 \quad \text{.....(10)}$$

$$P_c2(S_w) = -10 * S_w + 10 \quad \text{.....(11)}$$

$$P_c3(S_w) = -20 * S_w + 20 \quad \text{.....(12)}$$

$$P_c4(S_w) = \frac{2.8}{\tan(\pi * S_w - \pi)} + 12 \quad \text{.....(13)}$$

$$P_c5(S_w) = \frac{0.22}{\left(S_w - S_{w_{irr}}\right)^{1.4}} \quad \text{.....(14)}$$

$$P_c6(S_w) = p_d \left(\frac{S_w - S_{wirr}}{1 - S_{wirr}}\right)^{-\frac{1}{\lambda}} \quad \text{.....(15)}$$

$$P_c7(S_w) = \frac{\left(\left(\frac{S_w - S_{wirr}}{1 - S_{wirr}}\right)^{-\frac{1}{m_d}} - 1\right)^{\frac{1}{n_d}}}{\alpha_d} \quad \text{.....(16)}$$

Eq. 14 is in the format of the modified *J*-Function proposed by El-Khatib (El-Khatib 1995). Eqs. 15 and 16 are Brooks and Corey function, and van Genuchten function, respectively, from Gerhard and Kueper (2003).

Figure 3 shows some examples of how capillary pressure and water saturation can be modeled. Each method of modeling capillary pressure and water saturation has unique qualities that can be used to interpret fluid behavior in reservoirs. Characteristics to observe are that the slopes of Pc1, Pc2, and Pc3 (linear fits) are increasingly greater, that Pc4 (tangent fit) never reaches full water saturation at zero capillary pressure, and that Pc5 (El-Katib fit) never reaches zero capillary pressure while in the domain of possible water saturations.

The fit of the capillary pressure and water saturation will determine the

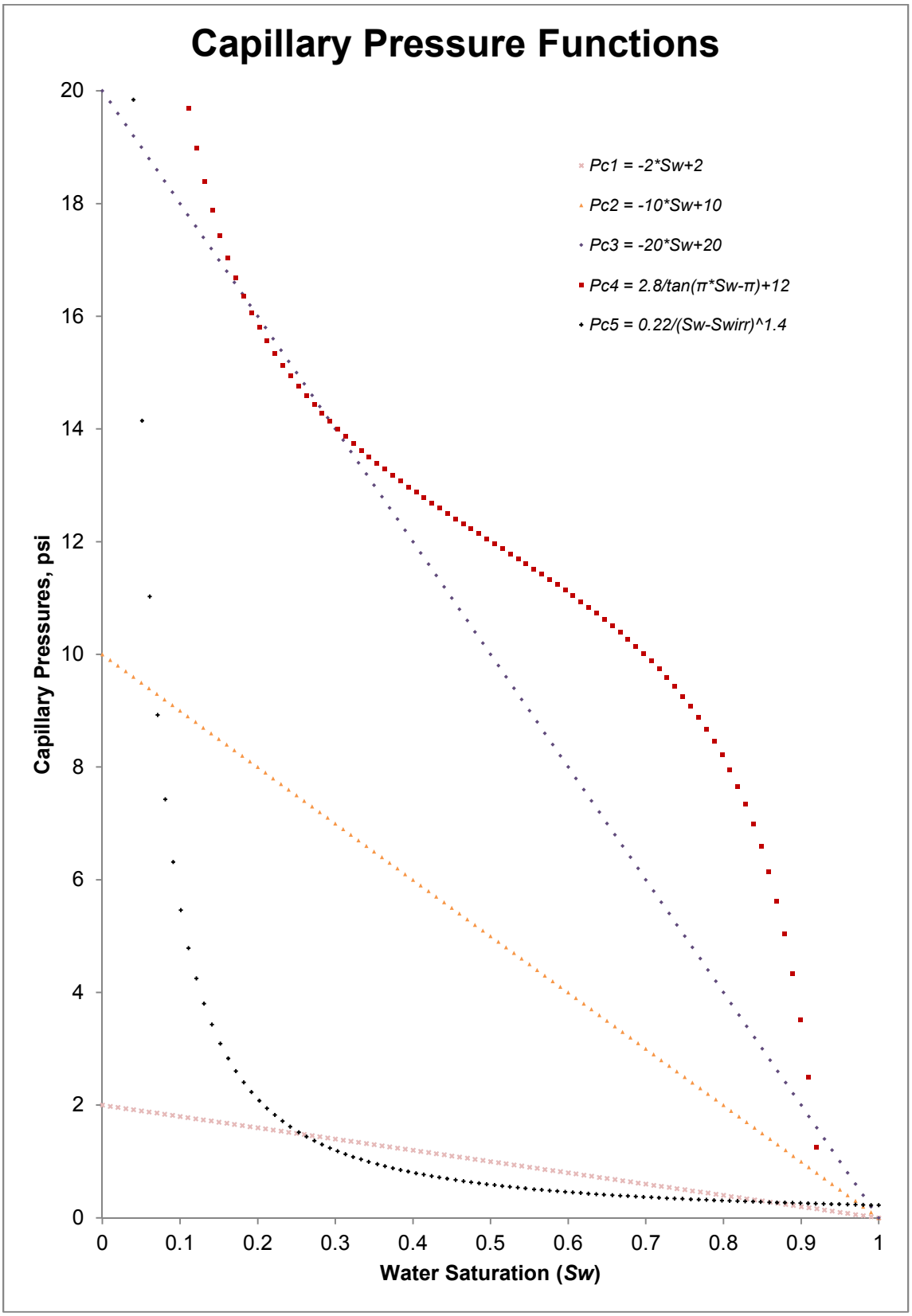

Figure 3: Basic Shapes of Capillary Pressure Functions ($P_c(S_w)$). Linear, tangent, and power law fits are shown.

estimates of oil saturation throughout the reservoir. Caution should be taken when basing reservoir fluid estimates when minimum fluid rock characterization has been done.

Figure 4 shows fits for capillary pressure-saturation functions. Pc5 is used as a reference. Pc6HO and Pc7HO are heavy oil fits for Pc6 and Pc7, respectively. The curvature and slope parameters were simplified for basic understanding of the shape of the functions.

Once the capillary pressure is fitted to an equation, then the saturation for any corresponding depth can be calculated by using the fitted equation. If the petroleum system has water, oil, and gas, there are three saturations with two of them independent and the third dependent on the others. The third saturation is calculated using a volumetric pore balance as seen in Eq. 17.

$$S_o + S_w + S_g = 1 \quad \text{.....(17)}$$

where S_o is the oil saturation, S_w is the water saturation, and S_g is the free gas saturation. S_g is zero below the gas-oil contact or if the reservoir is above the oil's bubble point pressure. This relationship can be made simpler if there is less than three phases (e.g., no free gas), or it can be made more complicated if there are more than three phases.

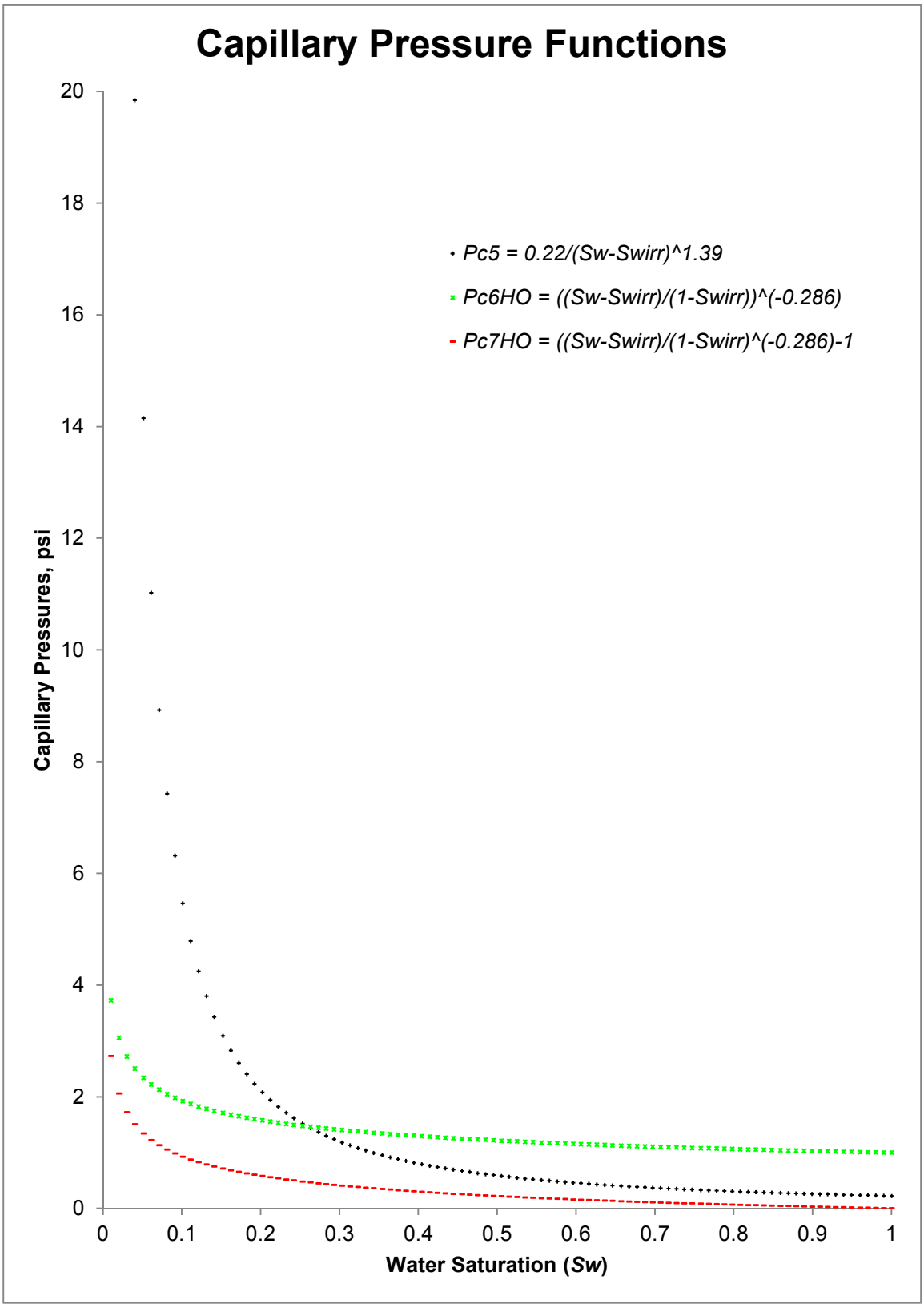

Figure 4: More Commonly Used Capillary Pressure Functions (*Pc(Sw)*). El Khatib, Brooks and Corey, and van Genuchten fits are shown.

CHAPTER 3

RESULTS

A good initialization model must have the capacity to have oil on top or oil on bottom depending on the density of the oil, to assimilate capillary pressure versus saturation data, and to predict fluid saturations. The developed one dimensional model is able to predict the initial saturations of a reservoir vertical column and can be used to initialize a geologic model for flow simulations.

Before looking at how saturation changes with depth, a capillary pressure function must be chosen or established. Capillary pressure-saturation functions research is an ongoing area of study and the equations and statistical modeling are becoming more and more complex, but for simplicity, this paper uses the basic functions (see Eqs. 10 – 14) to illustrate a few key factors of the capillary pressure-saturation functions that influence saturation-depth profiles (e.g., the extent of transition zones is proportional to the slow in the capillary pressure-saturation functions).

The first validation steps were taken in the most basic capillary pressure-saturation fitting functions (linear and tangent). The comparison between the developed model and the model imbedded into STARS software is nearly exact (as seen in Figure 5 and Figure 6). The solid lines in the plots represent the

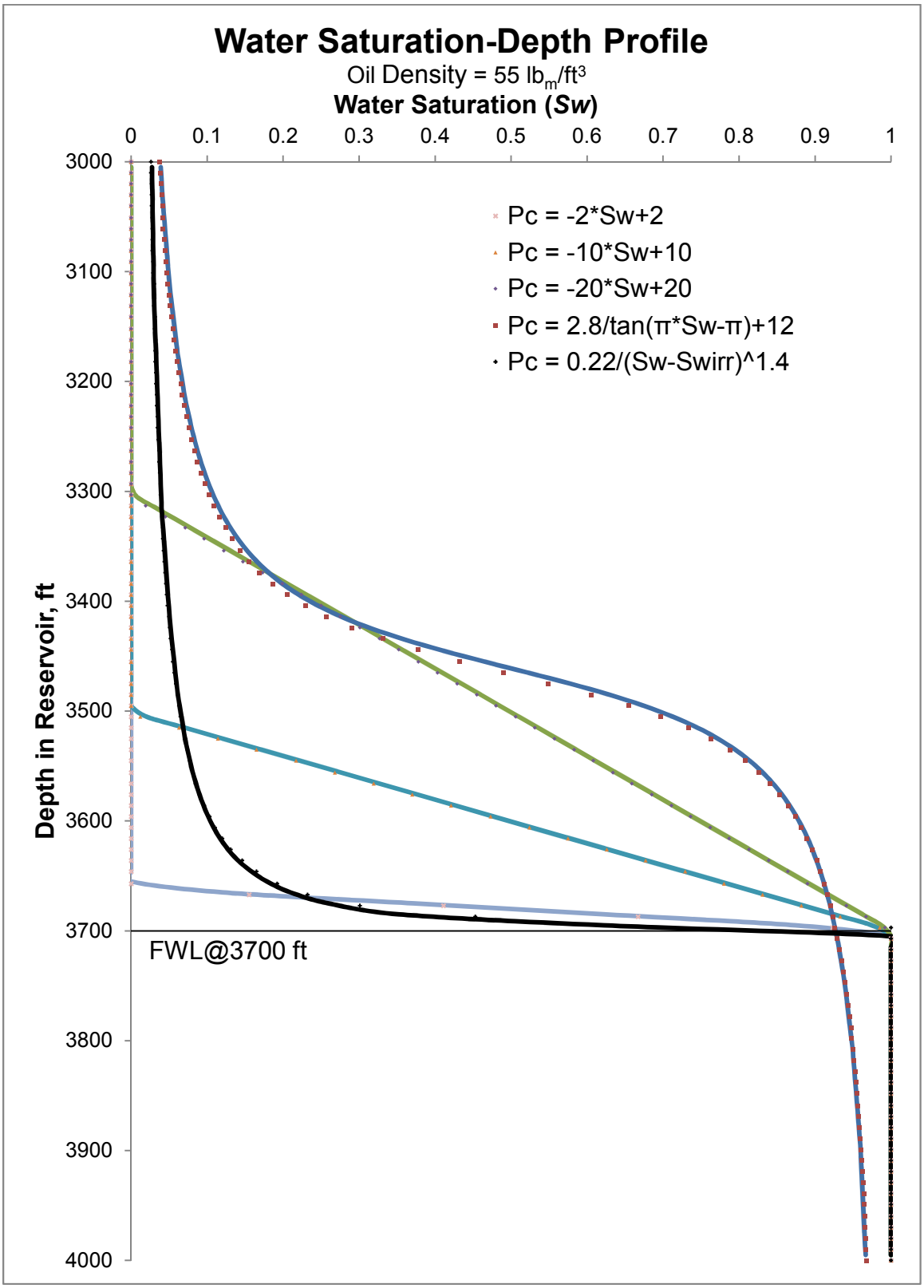

Figure 5: Oil-on-Top Saturation vs. Depth Scenario. Where the oil is less dense than water (62.4 lb_m/ft^3) using different capillary pressure-water saturation functions. Free water level (FWL) at 3700 ft.

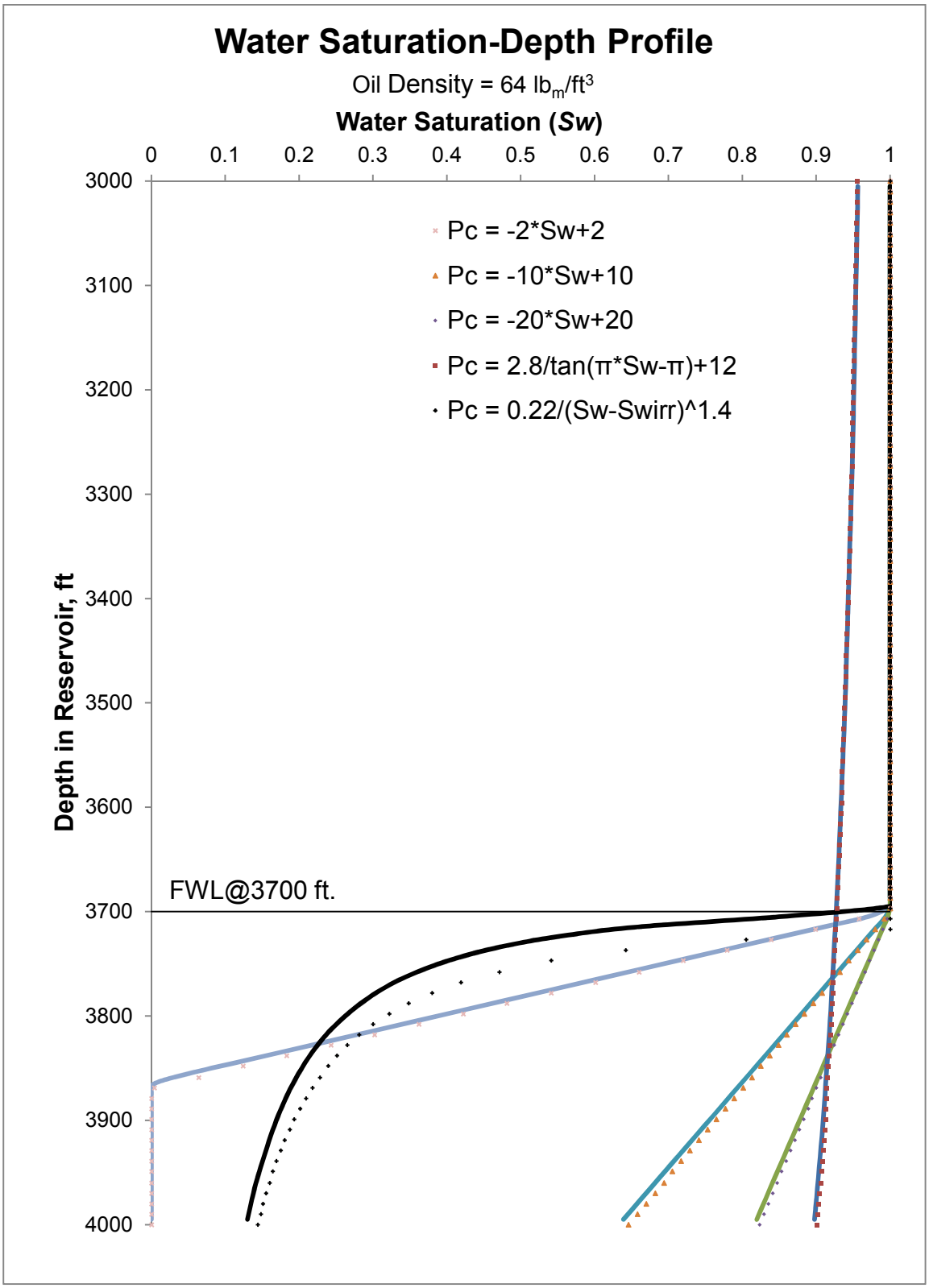

Figure 6: Oil-on-Bottom Saturation vs. Depth Scenario. Where the oil is denser than water (62.4 $lb_m/ft.^3$) using different capillary pressure-water saturation functions. Free water level (FWL) at 3700 ft.

STARS simulation results and the markers represent the developed model's results. The two different oil densities show an oil-on-top scenario and an oil-on-bottom scenario.

Figure 5 shows a comparison between the framework developed and the framework used in the commercial CMG software. The figure shows a case of conventional oil-lighter-than-water reservoir model with oil with a constant density and a free water level at 3700 feet.

In Figure 5, the capillary pressure functions (*Pc*1 to *Pc*5) have slopes and curvatures that are proportional to those seen in Figure 3. In the case of the linear fitted capillary pressure and saturation, the slopes from Eqs. 10 – 12 and the corresponding height of transition zones in Figure 5 are proportional. In the case of the tangent fitted function, the top and bottom reservoir characteristics have inherent residual water and oil saturations, thus there is no free water level. Finally, in the case of the power law fit, at the top of the reservoir the water saturation never reaches zero and at the bottom of the reservoir the free water level is not the same as the oil-water contact. The free water level (where $Pc = 0$) is set at 3700 feet and the oil-water contact is at 3696 feet

Figure 6 shows a comparison between the framework developed and the framework used in the commercial CMG software for the case in which oil is heavier than water. The same free water level (3700 ft) was used but in this case the water saturation diminishes below the contact.

In Figure 6, the capillary pressure functions (*Pc*1 to *Pc*5) have slopes and curvatures that are proportional to those seen in Figure 3. The slopes and

curvatures in Figure 5 do not match those in Figure 6 because of the relative density difference. In Figure 5, the density difference is 7.4 lb_m/ft^3 whereas in Figure 6 the density difference is 1.6 lb_m/ft^3. The implication of having a smaller density difference is that the transition zones will be more vertically extensive.

As seen in Figure 5 and Figure 6, the fit between the two models is nearly exact. The developed model, in addition to the conventional simulator models, takes the density as a function that is coupled with depth of the reservoir and is able to predict saturations through the free water level. The density function in this case is a linear change of $9.0*10^{-3}$ $lb_m/ft^3/ft$ (ranging from 55 to 64 lb_m/ft^3). This density gradient is greater than a density gradient from oil compressibility which ranges from $9.3*10^{-7}$ $lb_m/ft^3/ft$ to $5.9*10^{-5}$ $lb_m/ft^3/ft$. The developed model exaggerates this density change in the reservoir and the results increase theoretical understanding. As seen in Figure 7, if the oil density were to change at the rate set, then there is a possibility of having two free water levels where the capillary pressure equals to zero, which translates into potential heavy oil to be found under the free water level in a reservoir. The two transition zones are dependent on the capillary pressure and water saturation profiles of the fluid and rock. These transition zones are a determining factor if the heavy oil is producible.

Two- and three-phase systems allow for a fundamental look at how the saturations change throughout the reservoir with a varying oil density, but a gas phase exists in many reservoirs. Gas phase was modeled with an input of a gas-oil contact and a change to the capillary pressure equation from water saturation

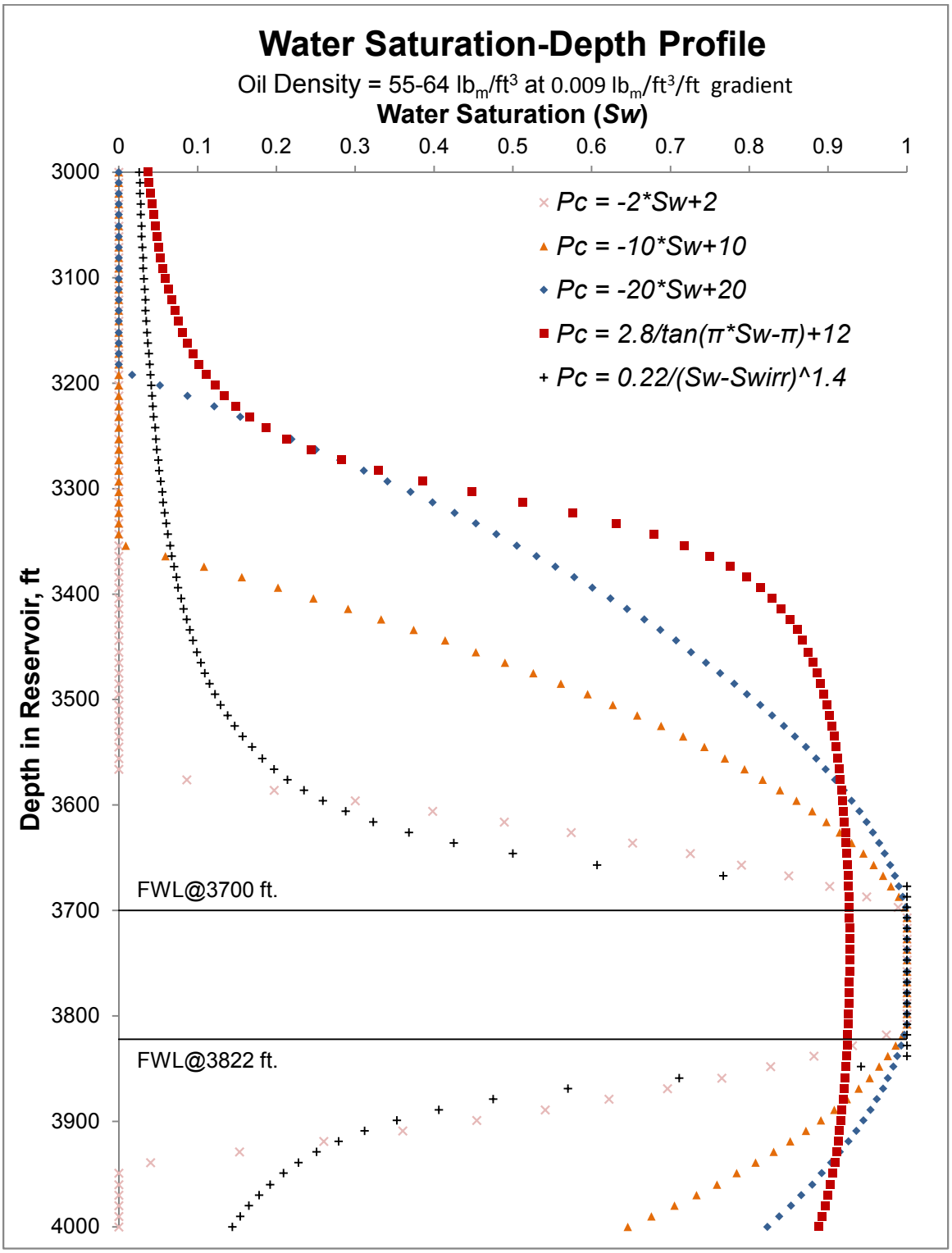

Figure 7: Two Oil-Water Contacts Saturation vs. Depth Scenario. Where the oil is on top and on bottom. The hypothetical oil has a constant oil density gradient starting less dense than water transitioning into a denser-than-water oil. Free water levels are found at 3700 ft and 3822 ft.

(S_w) to liquid saturation (S_l). In the hypothetical model of separate oleic phases the system exhibits four phases with heavy and light oil being two distinct phases.

Figure 8, Figure 9, and Figure 10 each show three-phase models with a linear oil density gradient and capillary pressure models of El-Khatib (*Pc*5), Brooks and Corey (*Pc*6), and van Genuchten (*Pc*7). The gas oil contact (GOC) is set at 3200 ft and the free water level (FWL) is set at 3700 ft. The depiction would be typical of an oversaturated reservoir (with a gas cap). This type of reservoir is theoretical because having the two extremes in oil is not likely to occur without great temperature instability in situ, selective biodegradation, or some other phenomenon, but for the purpose of increasing understanding the possibility is explored.

Figure 8 uses the same capillary pressure-saturation profile for all the phases. This was done to demonstrate the interactions between the phases. The capillary pressure-saturation profile can be seen in Figure 3 as *Pc*5.

In Figure 8, the rapid decrease of oil above the GOC has the same characteristics as the comparison between the oil transitions in Figure 5 and Figure 6. It is seen more sharply in Figure 8 because the density difference between the liquid phase and gas phase is even larger than the density difference between the heavier-than-water oil and lighter-than-water oil cases.

Figure 9 shows a Brooks and Corey model using Eq. 15 with a constant density gradient of 0.009 $lb_m/ft^3/ft$ (ranging from 55 to 64 lb_m/ft^3). Figure 9 is a more realistic model of the phases because each phase has its own capillary

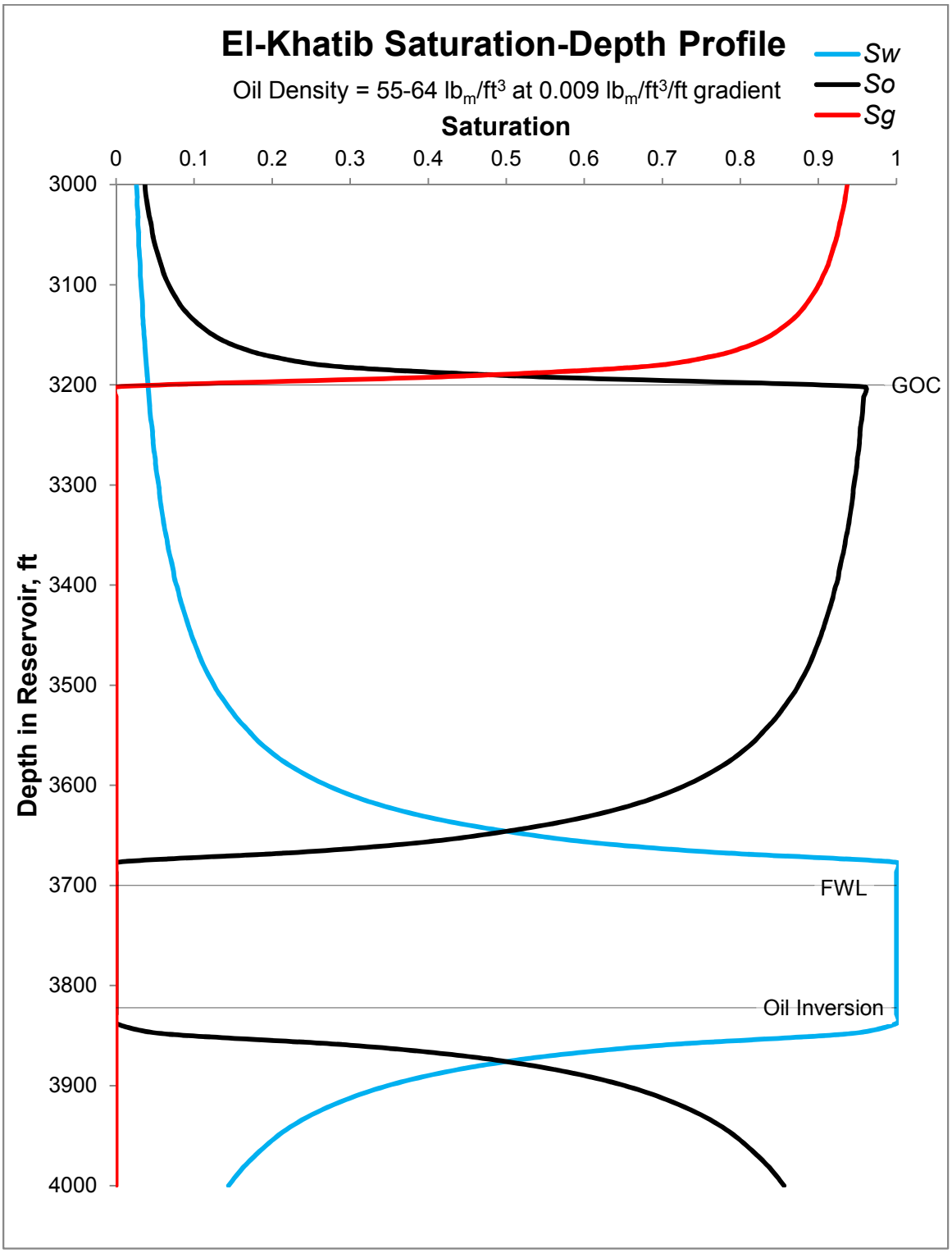

Figure 8: El Khatib Three-Phase Saturation vs. Depth Profile. Using capillary pressure fitting function proposed by El-Khatib with a constant oil density gradient. Free water levels are found at 3700 ft (FWL) and 3822 ft (Oil Inversion).

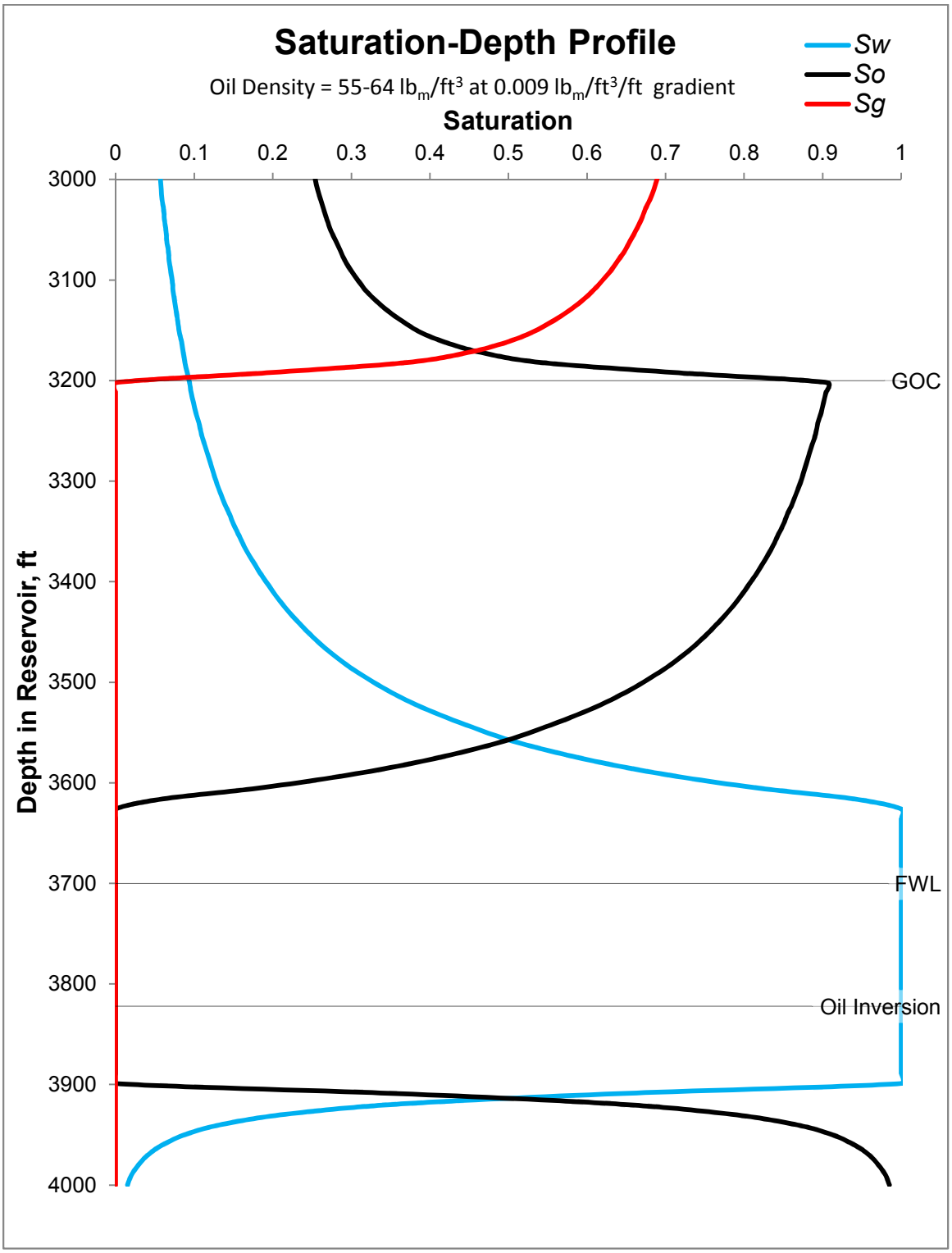

Figure 9: Brooks and Corey Three-Phase Saturation vs. Depth Profile. Capillary pressure-saturation fit with *Pd* = 1 and λ = 0.3, 0.8, and 3.5 for gas, light oil, and heavy oil, respectively. Free water levels are found at 3700 ft. (FWL) and 3822 ft. (Oil Inversion).

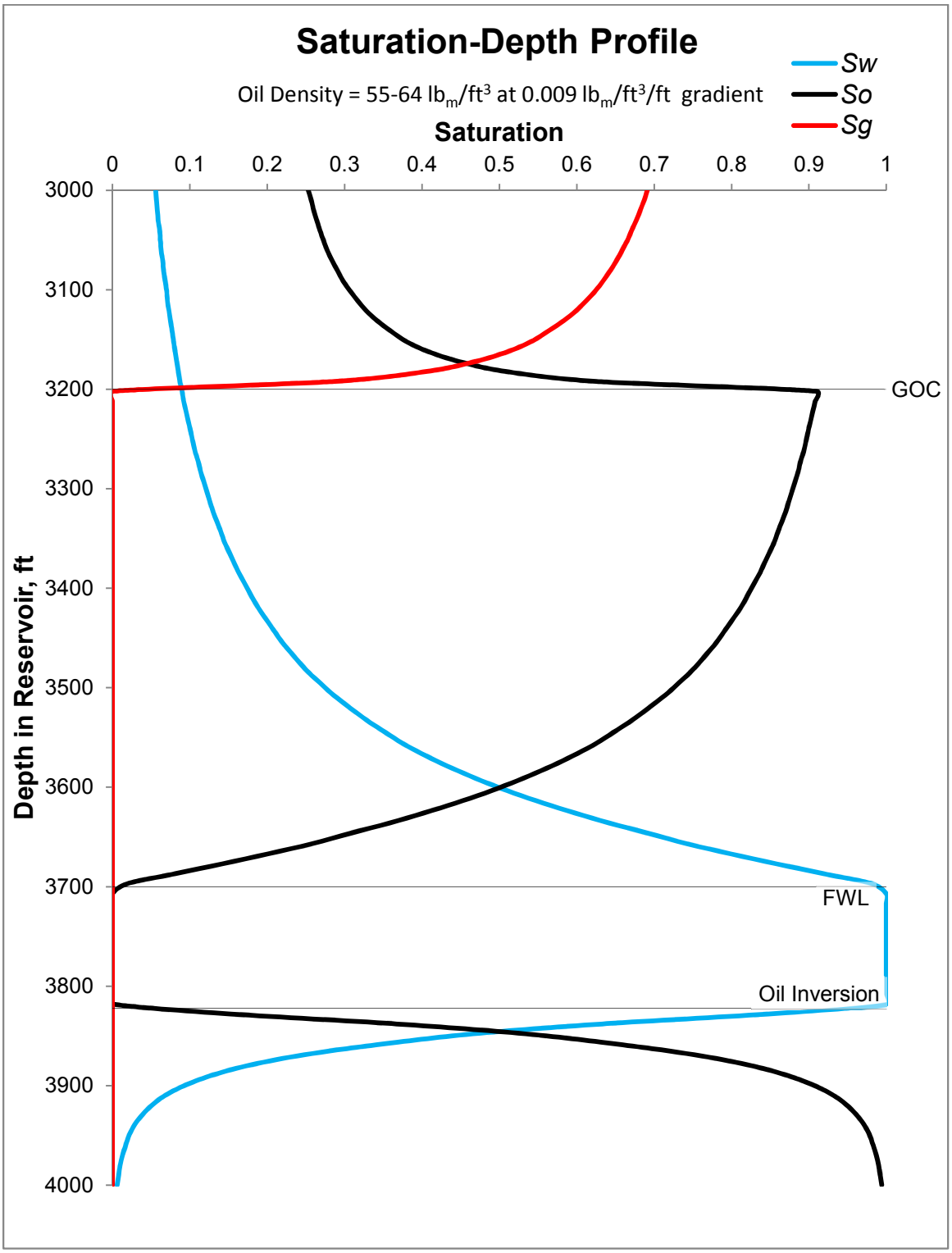

Figure 10: van Genuchten Three-Phase Saturation vs. Depth Profile. Capillary pressure-saturation fit with n_d = 1, α_d = 1 and m_d = 0.3, 0.8, and 3.5 for gas, light oil, and heavy oil, respectively. Free water levels are found at 3700 ft (FWL) and 3822 ft (Oil Inversion).

pressure-saturation function. From Eq. 15, only λ changed in the equation for each phase (i.e., λ equaled 0.3, 0.8, and 3.5 for gas, light oil, and heavy oil, respectively). It would be likely that more than one parameter would change between the different phases but the added curvature complexity doesn't add value in support of this thesis.

In Figure 9, the distinct difference is clear between FWL and OWC. This characteristic reservoir behavior is reflected in Figure 4, in which Pc6 does not reach zero within the realistic saturation range. The heavy oil transition zone is much sharper than the other transition zones. This is related to the proportionality of the slope in the capillary pressure-saturation profile. This characteristic was also evident in the linear cases in Figure 5. The pattern of larger transition zones for the density differences can also be observed. With a depth-dependent oil density, the transition zones vertically extend at the extremes of the density difference. This pattern is somewhat obscured by the end behaviors of the capillary pressure-saturation profile, but it is still present in Figure 9.

Figure 10 shows a van Genuchten model using Eq. 16 with a constant density gradient of 0.009 $lb_m/ft^3/ft$ (ranging from 55 to 64 lb_m/ft^3). Similar to Figure 9, the model was simplified by only changing one input parameter into the model. To allow for comparisons between Figure 9 and Figure 10, the analogous parameter to λ, m_d, was changed between the phases (i.e., m_d equaled 0.3, 0.8, and 3.5 for gas, light oil, and heavy oil, respectively).

In Figure 10, the FWL and OWC were at the same point. This is due to the capillary pressure-saturation profile crossing the *x*-axis at a saturation of 1. The

same transition zone extent changes between the phases can be seen as in Figure 9.

Figure 11 shows a water saturation profile (simplified van Genuchten, i.e., m_d = 1, n_d = 1, and α_d = 1) with a step change in the oil density at the oil-water contact (3500 ft) from 60.8 to 64 lb_m/ft^3 and heterogeneous permeability. The input of density and permeability alter the capillary pressure function as seen in Eqs. 8 and 9. The *J* value in Eq. 9 is calculated from Layer 4. The density of the lighter-than-water oil is 60.8 lb_m/ft^3 and the density of the heavier-than-water oil is 62.4 lb_m/ft^3. The free water level is set at 3500 ft. A reference homogeneous permeability reservoir is shown for comparison.

In Figure 11, the FWL and OWC are the same because the van Genuchten fit crosses the *x*-axis at a water saturation of 1. The permeability demonstrates a positive correlation with oil saturation (e.g., greater permeability than basis equates to greater oil saturation). The change in permeability effectively changes the capillary pressure function by a factor of the ratio of the square roots of permeability at basis and new permeability (e.g., $Pc_{layer7}(Sw) = Pc_{layer5}*\sqrt{10}/\sqrt{100}$).

Figure 12 shows a step change in the oil density at the oil-water contact (3500 ft) from 60.8 to 64 lb_m/ft^3 and heterogeneity in porosity. Similar to Figure 11, the figure uses the van Genuchten equation for the capillary pressure saturation curve and Eqs. 8 and 9 to adapt the equations to the reservoir characteristics. Layer 4 is the basis for the Eq. 8 and the FWL is at 3500 ft. The density of the lighter-than-water oil is 60.8 lb_m/ft^3 and the density of the heavier-

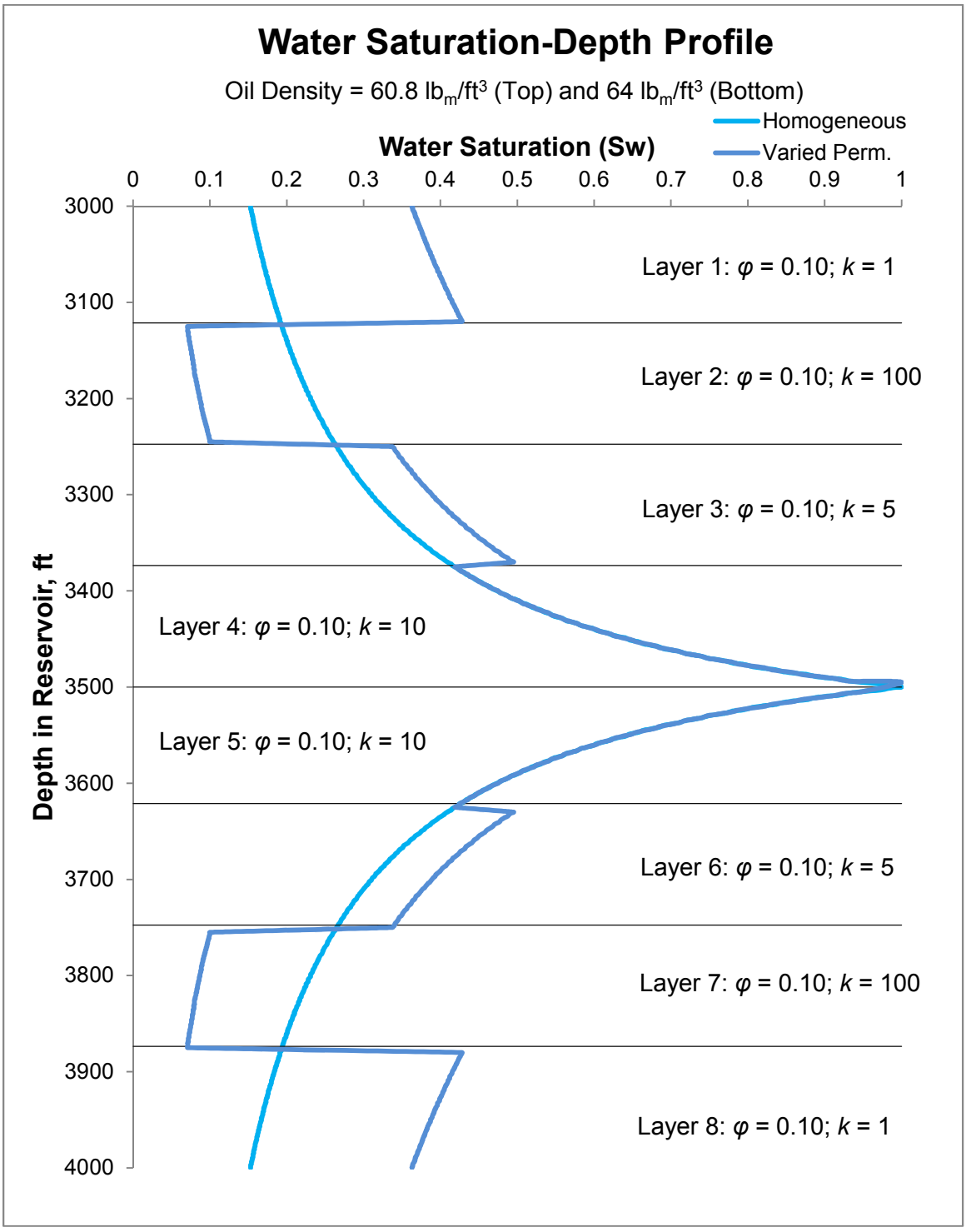

Figure 11: Water Saturation vs. Depth Profile in Heterogeneous Permeability. Profile being altered by varied permeability within a reservoir using a *J*-function comparison. Layer 4 and Layer 5 are used as the reference porosity and permeability (millidarcy). The van Genuchten saturation fit with n_d = 1, α_d = 1 and m_d = 1 was used for the basis capillary pressure function.

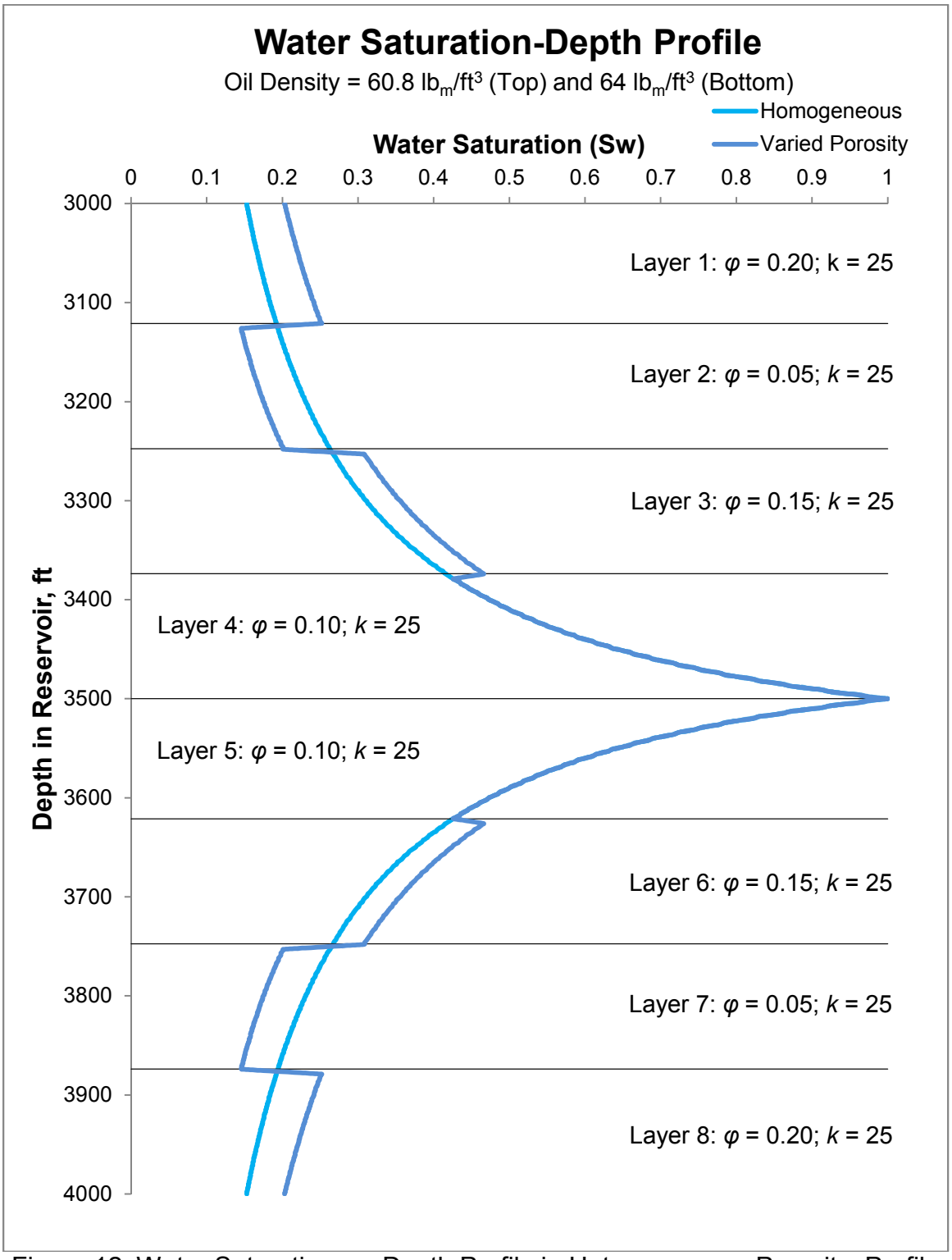

Figure 12: Water Saturation vs. Depth Profile in Heterogeneous Porosity. Profile being altered by varied porosity within a reservoir using a *J*-function comparison. Layer 4 and Layer 5 are used as the reference porosity and permeability (millidarcy). The van Genuchten saturation fit with n_d=1, α_d=1 and m_d=1 was used for the basis capillary pressure function.

than-water oil is 62.4 lb_m/ft^3.

In Figure 12, the porosity demonstrates a negative correlation with oil saturation (e.g., less porosity than basis equates to greater oil saturation). Like permeability, change in porosity effectively changes the capillary pressure function by a factor of the ratio of the square roots of new porosity and basis porosity (e.g. $Pc_{layer7}(Sw) = Pc_{layer5}*\sqrt{0.05}/\sqrt{0.10}$). The factor of porosity is less intense than the factor of permeability if the two were uncoupled.

Figure 13 shows a three-phase model with an oil density gradient of 0.009 $lb_m/ft^3/ft$, ranging from 55 to 64 lbm/ft^3) and heterogeneity in permeability. Similar to Figure 10, the different phases each have a separate capillary pressure-saturation van Genuchten fitted capillary pressure-saturation profile. The FWL is at 3700 ft. The basis for Eq. 9 was Layer 4 (3400 to 3500 ft). Oil Inversion is at 3822 ft based on when oil density is equal to water density (62.4 lb_m/ft^3).

In Figure 13, a combination of all the previous factors that can influence the saturations can be seen. The first 200 ft of the reservoir is a gas cap. At 3100 ft there is an unconformity where the permeability changes from 1 md to 100 md. Using Eq. 9 to model the change in layers of similar rock properties, saturation shifts can be observed. The reservoir fluid static behavior is modeled by the van Genuchten capillary pressure and saturation model. The lumping of capillary pressure-saturation profiles into heavy oil (m_d = 3.5), light oil (m_d = 0.8), and gas (m_d = 0.3) categories is better than assuming one equation for all of them, but still has uncertainty as the oil density characteristics are changing with depth.

Transition zones with water heavier and lighter than oil have been shown

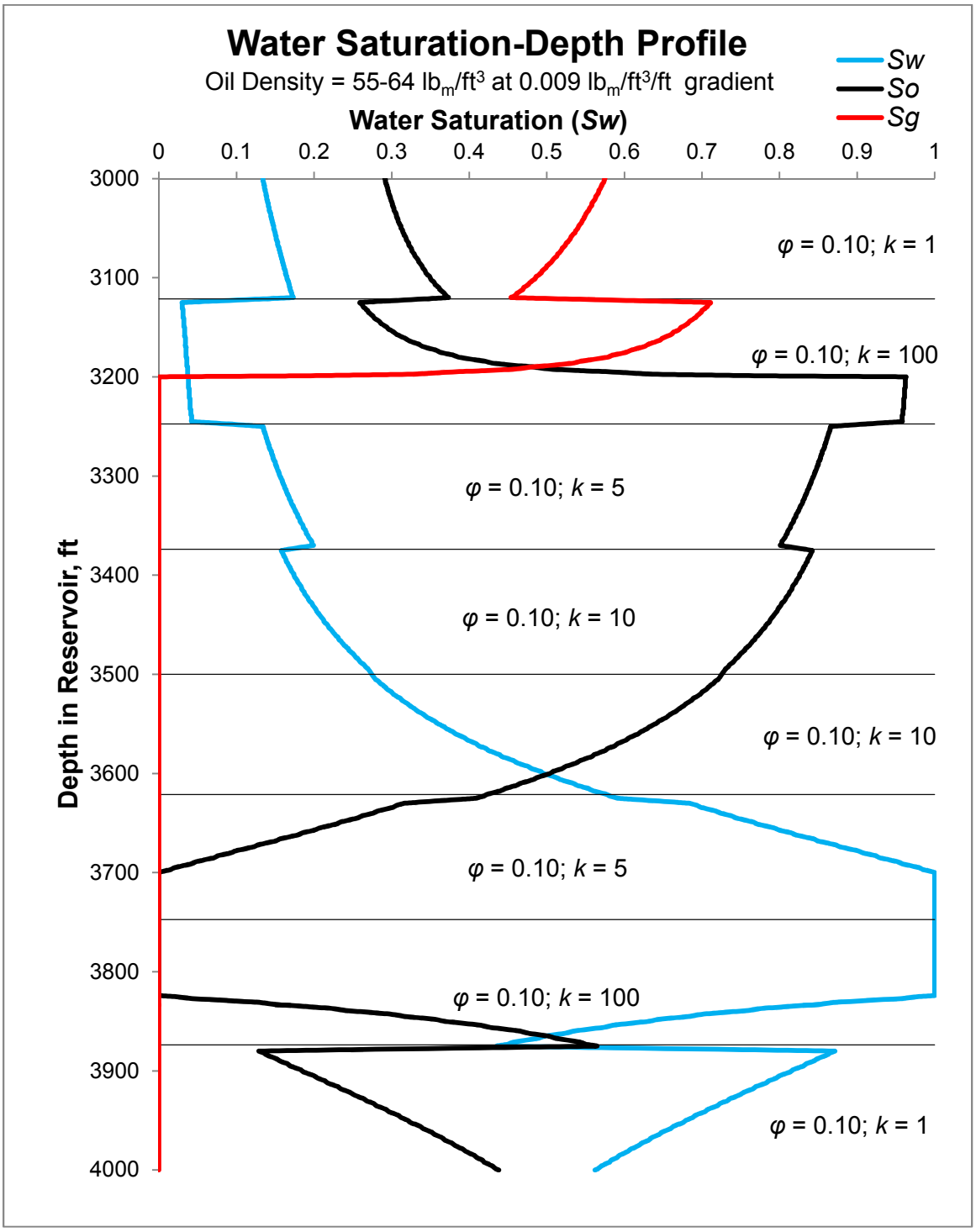

Figure 13: Three-Phase Saturation vs. Depth Profile in Heterogeneous Permeability. Profile being altered by varied permeability within a reservoir using a *J*-function. Layer 4 and Layer 5 are used as the reference porosity and permeability (millidarcy). The van Genuchten saturation fit with n_d=1, α_d=1 and m_d=0.3, 0.8, and 3.5 for gas, light oil, and heavy oil, respectively, was used for the basis capillary pressure function.

for different capillary pressure-saturation profiles. If there were a density gradient that bridged the two types of oils, there would be two separate oil water contacts. Three-phase systems were explored for different capillary pressure functions to describe how the capillary pressure functions alter the curvature of the saturation-depth profile. Finally, reservoir heterogeneity is introduced into the model.

CHAPTER 4

DISCUSSION

An exploratory model to understand the relationship of capillary pressure versus water saturation and depth and water saturation was developed using different function types (e.g., linear, tangent, El Khatib's function, Brooks and Corey's function, and van Genuchten's function) to discover what effects in the capillary pressure versus saturation relationships are coupled into the saturation versus depth profile. The comparison showed that the slope of the capillary pressure versus saturation profile, density difference, permeability, and porosity were proportional to the size of the transition zone and that the end behavior of the capillary pressure-saturation profile determines maximum possible saturation and whether the oil-water contact is the same as the free water level.

The model's results showed a possibility of two distinct oil-water contacts under certain conditions in oil reservoirs with a large oil density gradient. The theoretical reservoir has light oil on the top, water in the middle, and heavy oil on the bottom. The oil and water phase pressures are equal at the oil-water contacts, meaning that the capillary pressure is zero. There are two possibilities for Eq. 8 to equal zero. The first oil-water contact is at the depth where the water reaches full saturation, h_{owc} is set to zero. The second oil-water contact is at the

depth where the densities of water and oil are equal and the oil deeper than that point is denser than water. The two water contacts are at 3700 ft and 3822.22 ft and the change can be best seen in the van Genuchten fit (Figure 10) because the displacement pressure is 0 psi, whereas in the other models the displacement pressure is greater than zero. In this capillary pressure–depth model, thermodynamic relationships were not included; therefore, the gas-oil contact may not have physiological meaning, in that heavy oil reservoirs are unlikely to be saturated with gas, and therefore will have no free gas, but a GOC, at 3200 ft, is included for a nominal representation of the capillary pressure concept.

Capillary pressure-saturation functions must be coupled together through the reservoir where they may change (e.g., where the density of oil supersedes the density of water). The heavy-oil phase below the water zone and the light-oil phase above the water zone have different capillary pressure versus saturation profiles. Research has not adequately described the change in capillary pressure versus saturation profiles due to oil properties, most likely due to the complex nature of oil. Further research is required to determine if there is a need to have a more adjustable capillary pressure-saturation equation for density, viscosity, and interfacial tension changes by component distribution throughout a reservoir in addition to temperature and pressure differences.

The transition zones above the light oil-water contact (OWC1) and below the heavy oil-water contact (OWC2) have different rates of change (e.g., the transition zone of OWC2 has a smaller vertical extent than OWC1). Each

reservoir has a unique capillary pressure versus saturation relationship, but some generalizations can be made when laboratory data are not available. The developed code has the breadth to use heuristics or laboratory data to model a reservoir's saturation profiles.

In the model the oil density gradient is a linear function of depth. This demonstrates the concept that if the densities were to invert in the reservoir, there would be a second oil-water contact in which the capillary pressure was zero. The constant oil density gradient is theoretical and not seen in reservoirs, but it is interesting that with a dense phase changing from water to oil, the oil phase is seen to pool instead of float. The model has other weaknesses such as homogeneity and a large depth extent, but as a theoretical demonstration of what may occur if all other variables were kept constant and density were to change, the model shows a clear reemergence of oil at the bottom of the reservoir.

Cross software validation was performed. Results indicate that the model will be representative of most heavy oil reservoirs. The validation compared the model in this paper to a state-of-the-art software package from Computer Modeling Group Ltd. (STARS). The code will be transcribed into the reservoir initialization section in the University of Utah's implicit reactive transport simulator, Advanced Reactive Transport Simulator (ARTS). The plug-in for ARTS will aid in initializing petroleum systems which will increase accuracy and efficiency of each simulation.

There are two theoretical possibilities that may explain why there is oil below the oil-water contact. The first would be to have two charges of oil — the

first of heavy crude oil and the second of light crude oil. The second charge of light crude would precipitate asphaltenes, scrubbing the heavy oil of the light ends and forming a gas cap. The second possibility is that at the oil-water contact there are bacteria that consume the light ends, leaving only heavier-than-water compounds.

CHAPTER 5

CONCLUSIONS

The results of the proposed model lead to an unforeseen potential hazard in heavy oil reservoir modeling and production. A water gap hazard could lead to a well's failure to produce oil. The saturation profile model with two oil phases can forewarn against the water gap hazard.

Accurate saturation profiles are the first step in providing a fully compositional model that will describe oil components versus depth for different reservoirs. Asphaltene gradients will be an essential construct in describing heavy oil reservoirs compositionally. A fully compositional simulator will need an equation of state (EOS) that will describe asphaltene and other heavy oil component behavior. Once all of the pieces of the compositional model are in place, it will be a powerful tool for service and energy companies to increase production while minimizing their environmental impact.

The need for an accurate description of saturations in a reservoir is becoming more evident as enhanced oil recovery methods are being implemented. In steam-injection recovery, water saturation can become a detriment to ultimate recovery as well as overall efficiency. Both efficiency and

ultimate recovery influence the monetary value and environmental impact of each well in the field that is being developed.

REFERENCES

Brooks, R. H. and Corey, A. T. 1964. Hydraulic Properties of Porous Media. *Hydrology Papers* **3**. Colorado State University, Fort Collins, Colorado (March 1964).

El-Khatib, N. 1995. Development of a Modified Capillary Pressure *J*-Function. *Proc.*, SPE Middle East Oil Show, Bahrain, 11-14 March, SPE-*29890*, 547–562.

Gerhard, J. I. and Kueper, B. H. 2003. Capillary Pressure Characteristics Necessary for Simulating DNAPL Infiltration, Redistribution, and Immobilization in Saturated Porous Media. *Water Resources Research*, **39** (8): 1–17. http://doi.org/10.1029/2002WR001490.

Head, I. M., Gray, N. D., and Larter, S. R. 2014. Life in the Slow Lane; Biogeochemistry of Biodegraded Petroleum Containing Reservoirs and Implications for Energy Recovery and Carbon Management. *Frontiers in Microbiology **5*** (Article 566). http://doi.org/10.3389/fmicb.2014.00566

Hein, F. J., Leckie, D., Larter, S., and Suter, J. R. 2013. Heavy Oil and Bitumen Petroleum Systems in Alberta and Beyond: The Future Is Nonconventional and the Future Is Now. *Heavy-Oil and Oil-Sand Petroleum Systems in Alberta and Beyond: AAPG Studies in Geology 64*, 1–22. Tulsa: AAPG, Canadian Heavy Oil Association, and AAPG Energy Minerals Division. http://doi.org/10.1306/13371576St643550

Høier, L., Whitson, C. H., and Pera, N. 2001. Compositional Grading — Theory and Practice, *SPE Res Eval & Eng* (December): 525–535, SPE-74714

Hondroyiannis, G., Lolos, S., and Papapetrou, E. 2002. Energy Consumption and Economic Growth: Assessing the Evidence from Greece. *Energy Economics*, ***24*** (4): 319–336. http://doi.org/10.1016/S0140-9883(02)00006-3

Lee, S. T. 1989. Capillary-Gravity Equilibria for Hydrocarbon Fluids in Porous Media. *Proc.*, SPE 64th Annual Technical Conference and Exhibition, San Antonio, Texas, 8–11 October, SPE-19650, 213–228.

Leverett, M. C. 1940. Capillary Behavior in Porous Solids. *Proc.*, Tulsa Meeting, October 1940, 152–169.

Muskat, M. 1930. Distribution of Non-Reacting Fluids in the Gravitational Field. *Physical Review **35***, 1384–1393.

National Renewable Energy Laboratory. 2015. Energy Analysis, http://www.nrel.gov/analysis/ (Accessed June 15, 2015).

Phelps, R. E. 1993. Lithology-Dependent *J*-Functions and Relative Permeabilities. *Proc.*, SPE Middle East Oil Technical Conference and Exhibition, Manama, Bahrain, 3–6 April, SPE-25661-MS, 525–536. http://doi.org/10.2118/25661-MS

Sage, B., and Lacey, W. 1939. Gravitational Concentration Gradients in Static Columns of Hydrocarbon Fluids. *Transactions of the AIME*: 120–131. SPE-939120-G. https://www.onepetro.org/journal-paper/SPE-939120-G

Sarwaruddin, M., Skauge, A., and Torsaeter, O. 2001. Modeling of Capillary Pressure for Heterogeneous Reservoirs By a Modified *J*-Function, Presented at Symposium of the Society of Core Analysts, Edinburgh, UK, 17–19 Setember. SCA 2001-35

Schulte, A. M. 1980. Compositional Variations Within a Hydrocarbon Column Due To Gravity. *Proc.,* SPE 55th Annual Fall Technical Conference and Exhibition, Dallas, Texas, 21–24, SPE-9235. http://doi.org/10.2523/9235-MS

Sedaghat, M. H., Daliri, A., and Mohammadi, H. 2013. Improvement of Whitson Algorithm for Chemical/Gravity Equilibrium Calculations to Compute Compositional Gradient in Petroleum Reservoirs. *Egyptian Journal of Petroleum* **22** (2), 305–311. http://doi.org/10.1016/j.ejpe.2013.06.009

Tidball, R., Bluestein, J., Rodriguez, N., and Knoke, S. 2010. Cost and Performance Assumptions for Modeling Electricity Generation Technologies. NREL/SR-6A20-48595, National Renewable Energy Laboratory, Golden, Colorado (November 2010). http://www.nrel.gov/docs/fy11osti/48595.pdf

U.S. Energy Information Administration. 2012. Annual Energy Review 2011. DOE/EIA-0384(2011), U.S. Department of Energy, Washington, DC (September 27, 2012).

U.S. Energy Information Administration. 2013. International Energy Outlook 2013. DOE/EIA-0484(2013), U.S. Department of Energy, Washington, DC (July 2013). http://doi.org/EIA-0484(2013)

van Genuchten, M. T. (1980). A Closed-form Equation for Predicting the Hydraulic Conductivity of Unsaturated Soils1. *Soil Science Society of America Journal*, ***44*** (5), 891–898. http://doi.org/10.2136/sssaj1980.03615995004400050002x

Wheaton, R. J. 1991. Treatment of Variations of Composition With Depth in Gas-Condensate Reservoirs. *SPE Res Eng*, **6** (2): 239–244. SPE-18267.

Whitson, C. H. and Belery, P. 1994. Compositional Gradients in Petroleum Reservoirs. *Proc.*, University of Tulsa Centennial Petroleum Engineering Symposium, Tulsa, Oklahoma, 29-31 August. SPE-28000, 443–459.